View metadata, citation and similar papers at core.ac.uk
brought to you by CORE
provided by Elsevier - Publisher Connector

Cell Stem Cell
Article

Dynamic Equilibrium and Heterogeneity of Mouse Pluripotent Stem Cells with Distinct Functional and Epigenetic States

Katsuhiko Hayashi,[1,2] Susana M. Chuva de Sousa Lopes,[1,2,3] Fuchou Tang,[1] and M. Azim Surani[1,*]
[1]Wellcome Trust Cancer Research UK Gurdon Institute, The Henry Wellcome Building of Cancer and Developmental Biology, University of Cambridge, Tennis Court Road, Cambridge CB2 1QN, UK
[2]These authors contributed equally to this work
[3]Present address: Hubrecht Institute, Uppsalalaan 8, 3584 CT Utrecht, The Netherlands
*Correspondence: as10021@mole.bio.cam.ac.uk
DOI 10.1016/j.stem.2008.07.027

SUMMARY

Embryonic stem cells (ESCs) are apparently homogeneous self-renewing cells, but we observed heterogeneous expression of Stella in ESCs, which is a marker of pluripotency and germ cells. Here we show that, whereas Stella-positive ESCs were like the inner cell mass (ICM), Stella-negative cells were like the epiblast cells. These states were interchangeable, which reflects the metastability and plasticity of ESCs. The established equilibrium was skewed reversibly in the absence of signals from feeder cells, which caused a marked shift toward an epiblast-like state, while trichostatin A, an inhibitor of histone deactelylase, restored Stella-positive population. The two populations also showed different histone modifications and striking functional differences, as judged by their potential for differentiation. The Stella-negative ESCs were more like the postimplantation epiblast-derived stem cells (EpiSCs), albeit the *stella* locus was repressed by DNA methylation in the latter, which signifies a robust epigenetic boundary between ESCs and EpiSCs.

INTRODUCTION

Mouse embryonic stem cells (ESCs) exhibit a degree of similarity with three different transient cell populations in the mouse embryo: the inner cell mass (ICM) of blastocysts, the epiblast cells of early postimplantation embryos, and primordial germ cells (PGCs), which includes expression of pluripotency marker genes, such as *Oct4* (Chambers and Smith, 2004; Pesce et al., 1998; Surani et al., 2007; Zwaka and Thomson, 2005). However, unlike the cells in vivo, ESCs retain pluripotency and exhibit the capacity for indefinite self-renewal, while the cells in vivo undergo differentiation according to a strict developmental program. As long as ESCs are cultured in an appropriate medium, such as the one containing leukemia inhibitory factor (LIF) and with either serum or bone morphogenetic protein 4 (BMP4), they can undergo self-renewal without compromising pluripotency (Ying et al., 2003). For this reason, ESCs are generally regarded as a homogeneous group of cells in the majority of studies.

However, the precise provenance of ESCs for which there is no strict in vivo equivalent remains to be fully elucidated. Based on some recent studies, it has been suggested that germ cells may be the closest in vivo equivalent of ESCs (Zwaka and Thomson, 2005), partly because expression of Stella has been reported in both mouse and human ESCs, albeit heterogeneously (Clark et al., 2004; Payer et al., 2006). Stella, a definitive marker of the germ cell lineage, is, however, first observed in preimplantation embryos. Thereafter, Stella is repressed in the epiblast (Payer et al., 2006; Sato et al., 2002) and subsequently re-expressed only following specification of PGCs (Payer et al., 2006). Other proteins such as Pecam1, Nanog, and SSEA1 also exhibit heterogeneous expression in undifferentiated ESCs (Chambers et al., 2007; Cui et al., 2004; Furusawa et al., 2004; Payer et al., 2006; Toyooka et al., 2008). Thus, while heterogeneity is a hallmark of ESCs, it remains to be fully elucidated how this is compatible with pluripotency and self-renewal.

In this study, we set out to investigate the nature of Stella-expressing cells in undifferentiated ESCs. We demonstrate that Stella-positive ESCs are closely related to the ICM and not to the epiblast or PGCs. Moreover, cultured under conditions that maintain pluripotency, the proportion of Stella-positive cells remained relatively constant, while they were able to reversibly convert to Stella-negative ESCs. Expression of *stella* is regulated by chromatin-based modifications in ESCs, which can respond to both the environmental and epigenetic cues. We propose that while undifferentiated ESCs undergo self-renewal, they are in a highly dynamic state as they continuously fluctuate between an ICM- and epiblast-like phenotype. By contrast, *stella* is robustly repressed by DNA methylation in pluripotent stem cells derived from postimplantation epiblast cells (EpiSCs), which do not readily revert to an ICM-like state.

RESULTS

The Population of Stella-GFP-Positive Cells Remains Relatively Constant

We previously generated two *stella-gfp* transgenic ESC lines (SH10.10 and BAC9) with different lengths of the *stella* flanking sequences coupled to a gene for green fluorescent protein (GFP) as the reporter (Payer et al., 2006). In these ESCs,

expression of Stella as well as of Stella-GFP was detectable only in a subset of ESCs (Figures 1A–1C). Similar heterogeneous expression of Stella was also confirmed in nontransgenic ESCs by immunsostaining (data not shown). Notably, cells with expression of Stella-GFP coincided significantly with those observed for endogenous Stella expression. For example, this was the case in 126 of 141 (89%) randomly chosen ESCs, although some Stella-positive cells were negative for Stella-GFP (5%), and some strongly Stella-GFP-positive cells (6%) expressed Stella only weakly. Fluorescence-activated cell sorting (FACS) consistently revealed that around 20%–30% of ESCs were Stella-GFP positive under our culture conditions, irrespective of the passage number (Figure 1D). However, the exact proportion of Stella-GFP-positive cells occasionally deviated from this range, as they are susceptible to slight differences in culture conditions (data not shown). These observations were made whether we used ESCs from *stella-gfp* BAC9 or from *stella-gfp* SH10.10 transgenic mice, except that the fluorescence activity of Stella-GFP in BAC9 ESCs was weaker (Figure 1D), which is most likely the result of the integration of a different copy number of transgenes in the genome. For convenience, we used *stella-gfp* SH10.10 ESCs in the rest of the studies described here.

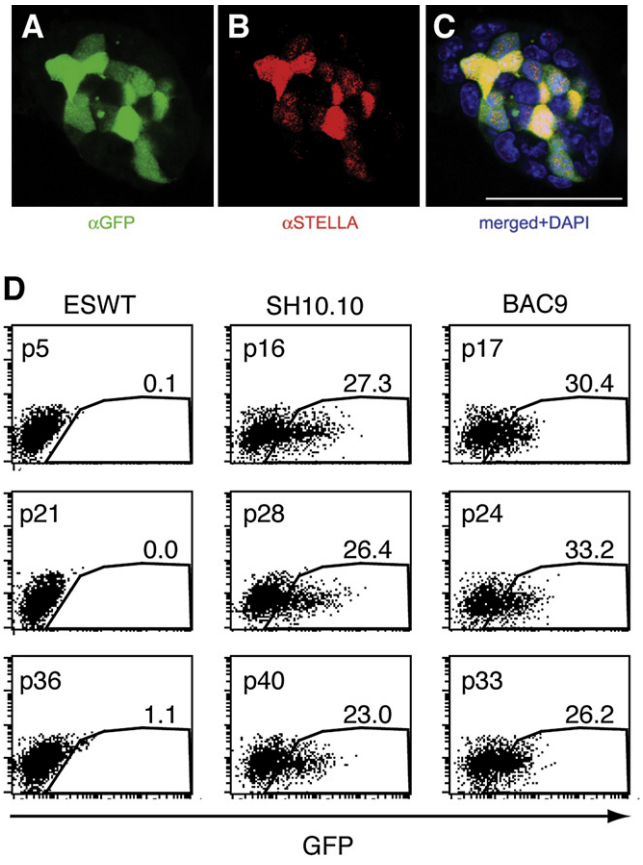

Figure 1. Heterogeneous Expression of Stella in Undifferentiated ESCs

(A–C) Immunoflurescence analysis of Stella-GFP (A) and endogenous Stella (B) expression in transgenic *stella-gfp* SH10.10 ESCs and their merged images with DAPI (C). Scale bar, 50 μm.

(D) Percentage of Stella-GFP-positive cells in control ces3 ESCs (ESWT; left), *stella-gfp* SH10.10 (middle), and *stella-gfp* BAC9 (right) transgenic lines. Numbers above the gates indicate the percentage of the GFP-positive cells plotted in each dot plot. Numbers described in upper left indicate the passage number.

Stella-GFP-Positive Population Is Enriched in ICM-Specific Markers

Next, we examined transcription profiles of the Stella-GFP-positive and -negative populations by quantitative reverse polymerase chain reaction (Q-PCR). Notably, we found that the two fractions clearly differed in the levels of expression of *Fgf5*, a marker of pluripotent epiblast cells of early postimplantation embryos, which is not expressed in the ICM (Pelton et al., 2002; Rathjen et al., 1999). Furthermore, *Gbx2* was also detected at a higher level in the Stella-GFP-negative cells, and like *Fgf5*, *Gbx2* is also upregulated in the primitive ectoderm cells soon after implantation (Figure 2A) (Chapman et al., 1997; Kurimoto et al., 2006). By contrast, the Stella-GFP-positive population was slightly enriched in *Pecam1* and *Zfp42/Rex1* transcripts, which are preferentially expressed in ICM compared to the epiblast (Figure 2A) (Pelton et al., 2002; Robson et al., 2001). Genes such as *alphafetoprotein* and *collagen type IV* that are upregulated in differentiated ESCs were not detectable in either of the two populations (data not shown), indicating that the Stella-GFP-negative population is not representative of differentiating ESCs.

Single-Cell Analysis

The above analysis was conducted on the two FACS-sorted cell populations, which would mask the extent of variations among individual cells. In addition, whereas Stella-GFP expression in ESCs showed extensive overlap with the endogenous expression of Stella, they do not coincide completely (Figures 1A–1C and 2A). Therefore, we decided to further investigate the nature of heterogeneity among the ESCs by examining gene expressions in 87 randomly selected single ESCs. Q-PCR analysis revealed variable *stella* transcripts in 63 (72.4%) cells (Figure 2B), among which we found 26 (29.9%) *Gfp*-expressing cells. Notably, *Gfp* was detected predominantly in cells with high expression of *stella* (Figure 2B), which is consistent with the 20%–30% of Stella-positive cells we detected by immunostaining. Among these, 15 of 26 cells showed high *stella* expression (*stella*-high; 57.8%), and 9 of 26 belonged to the *stella*-low group (34.6%) (Figure 2B). The differences in the percentage of cells with the *stella* transcript and those positive for the protein might be caused by translational regulation of *stella* transcript. It is possible that translational regulation is an important general feature of ESCs. Nevertheless, these results demonstrate that the number of *stella* transcripts in individual cells was variable, but virtually all the *stella-Gfp*-positive cells (92.9%, 26 of 28) were present within the group with high *stella* transcripts (Figure 2B).

Next, we extended our single-cell Q-PCR analysis to further assess expression of the other key marker genes. In agreement with the data from the FACS-sorted populations, we detected *Fgf5* expression predominantly among the *stella*-negative cells. By contrast, most *Pecam1*-expressing cells were among those with expression of *stella*, which also showed higher expression of *Zfp42/Rex1* (Figure 2B). Furthermore, it is of interest that expression of *Gbx2* was detected among the *stella*-low and *stella*-negative cells, which is consistent with the in vivo expression of *Gbx2* that starts to increase in the E4.5 primitive ectoderm

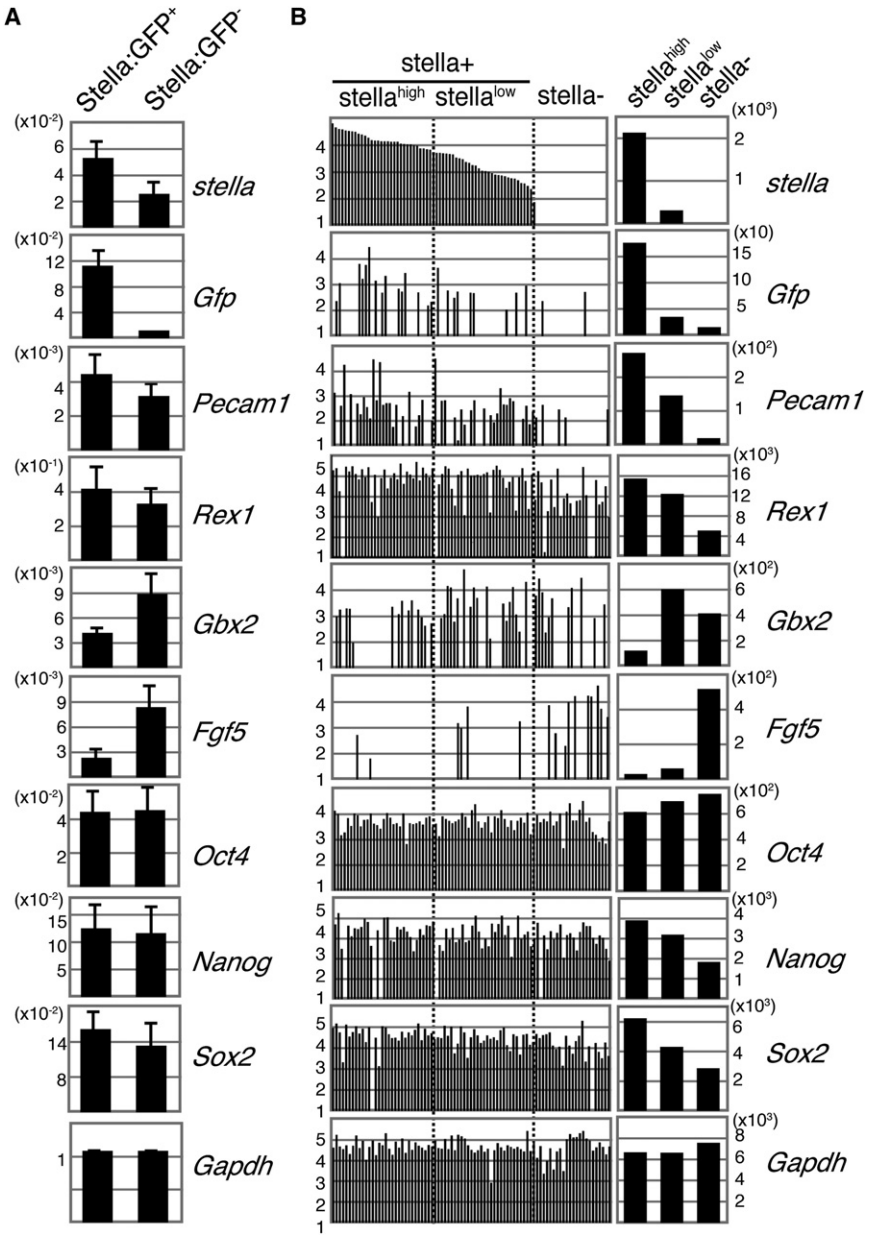

Figure 2. Differential Gene Expression in Stella-Positive and Stella-Negative Populations of *stella-gfp* SH10.10 ESCs

(A) Q-PCR analysis of each gene in FACS-sorted Stella-GFP-positive and Stella-GFP-negative populations. Relative levels of each gene expression are estimated by referring to the value of *Gapdh*. The mean values are calculated from three independent experiments.

(B) Q-PCR analysis using randomly selected single cells from *stella-gfp* ESCs. The left graph shows the putative number (log_{10}) of transcript in each single cell. Three populations, Stella^{high}, Stella^{low}, and Stella^{negative}, were identified and are set apart by broken lines. The right graph shows the average number of transcripts in each population.

at the time when *stella* expression begins to decline (Kurimoto et al., 2006). It is striking that the average numbers of *Nanog* and *Sox2* transcripts were also significantly lower in *stella*-negative cells compared to the *stella*-positive cells ($0.01 < p < 0.05$) (Figure 2B), which may reflect a decrease in these transcripts in vivo in the E4.5 primitive ectoderm and epiblast cells of mid-streak embryos, respectively (Avilion et al., 2003; Chambers et al., 2003). By contrast, *Oct4* transcripts were detected uniformly in all cells, which is the case in vivo in ICM and epiblast cells. Notably, these results indicated that the developmentally regulated genes are not expressed stochastically among ESCs, as their expression seems to reveal an adherence to the in vivo developmental program.

Consistent with the Q-PCR analyses of single cells, the entire population of Stella-GFP-positive ESCs was contained within the Pecam1-positive population by FACS analysis (see Figure S1 available online). *Pecam1* is a developmentally regulated gene that is homogeneously expressed in the ICM and completely absent from the epiblast (Figure S1 and Robson et al., 2001). This being the case, it is clear that the Stella-GFP-positive cells are contained within these ICM-like cells. By contrast, expression of SSEA1, which also shows heterogeneous expression in ESCs (Cui et al., 2004; Furusawa et al., 2004), was detected in both the Stella-GFP-positive and Stella-GFP-negative cells (Figure S1). However, unlike Pecam1, there is heterogeneous expression of SSEA1 in both the ICM and epiblast cells (Cui et al., 2004; Furusawa et al., 2004). We observed that the Stella-GFP-positive cells were detected within the SSEA1-positive as well as the SSEA1-negative population at comparable levels (17.4% versus 11.0%) (Figure S1). Immunofluorescence analysis confirmed that Stella-GFP-positive cells did not entirely overlap with the SSEA1-positive cells (Figure S1). These results again emphasize that heterogeneity among ESCs has a basis in the inherent developmental program in vivo.

The Subpopulations of ESCs Are Interchangeable

Next we asked how the relatively stable population of 20%–30% Stella-GFP-positive cells is maintained among the ESCs, for which there are at least two possibilities: either they are in a state of flux and interchange continuously between positive and negative states while maintaining a constant ratio, or they give rise only to descendants of the same type. To distinguish between these possibilities, FACS-sorted Stella-positive and Stella-negative ESCs populations were cultured and analyzed separately. To avoid contamination of cells that express endogenous *stella* but no *Gfp* transcripts, we used a Stella-GFP-negative/Pecam1-negative population, since single-cell analysis revealed

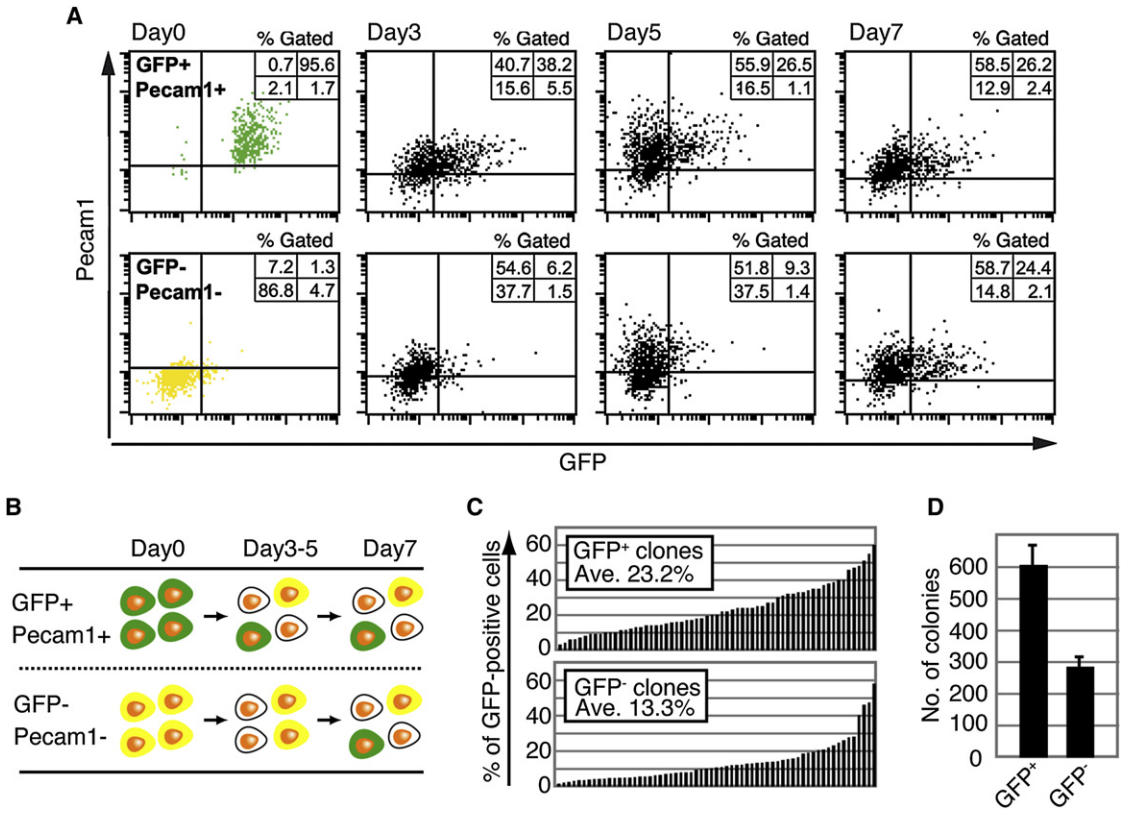

Figure 3. ESCs Display a State of Dynamic Equilibrium

(A) Stella-GFP-positive/Pecam1-positive (green) and Stella-GFP-negative/Pecam1-negative (yellow) FACS-sorted *stella-gfp* ESCs were cultured for 7 days. The percentage of cells with Stella-GFP expression was analyzed on days 0, 3, 5, and 7. Gating was determined independently at each time point using unsorted *stella-gfp* ESCs analyzed in parallel as a reference. The percentage of gated cells is given in the upper corner of each dot plot.

(B) Summary of phenotypic changes in Stella-GFP-positive/Pecam1-positive and Stella-GFP-negative/Pecam1-negative cells. Note that the Stella-GFP-positive/Pecam1-positive cells (green cells) revert to the original proportion more quickly than the Stella-GFP-negative/Pecam1-negative (yellow) cells. Cells depicted with white cytoplasm indicate Stella-GFP-negative/Pcam1-positive cells.

(C) Clonal analysis of Stella-GFP-positive/Pecam1-positive and Stella-GFP-negative/Pecam1-negative FACS-sorted *stella-gfp* ESCs. Cells were expanded for 9 days and the percentage of Stella-GFP-positive cells in each independent clone (n = 64) determined by FACS analysis. The averaged percentage is shown in each graph.

(D) Different rate of colony formation of Stella-GFP-positive/Pecam1-positive and Stella-GFP-negative/Pecam1-negative *stella-gfp* ESCs. The average numbers of colonies from Stella-GFP-positive/Pecam1-positive and Stella-GFP-negative/Pecam1-negative FACS-sorted *stella-gfp* ESCs are shown. The mean values are calculated from three independent experiments.

that cells that do not express endogenous *stella* were enriched within the double-negative population. Remarkably, after 3 days of culture, approximately 50% of the cells in both the individual fractions were found to be Stella-GFP negative/Pecam1 positive (Figure 3A). We consider these cells to be phenotypically closest to the two original isolated FACS-sorted populations described above. Indeed, these individual cultures were eventually fully restored to the original state of about 20%–30% Stella-GFP-positive cells that we first encountered among the *stella-gfp* ESCs. Interestingly, the Stella-GFP-positive/Pecam1-positive population reverted to the original state faster than the Stella-GFP-negative/Pecam1-negative cells, which occurred within 5 and 7 days of culture, respectively (Figures 3A and 3B). These results show that the FACS-sorted populations of ESCs representing the two extreme populations are interchangeable. Moreover, the two individual groups of cells first generated a large proportion of Stella-GFP-negative/Pecam1-positive cells, which were in turn followed by the generation of cell types that progressively departed further away from the original FACS-sorted Stella-GFP-positive/Pecam1-positive and Stella-GFP-negative/Pecam1-negative cell types, respectively. These observations suggest an adherence to an intrinsic program during their interconversion rather than a stochastic change in gene expression.

To exclude the possibility that the results could be influenced by the reciprocal contamination of the two cell populations, ESC subclones (n = 64) derived from FACS-sorted single Stella-GFP-positive/Pecam1-positive or Stella-GFP-negative/Pecam1-negative cells were analyzed at 9 days after FACS sorting. Clonal analysis revealed that both sets of cells could generate the reciprocal set of cells as in the parental cell lines (Figure 3C), except that there was a lower average percentage of Stella-GFP-positive cells detected from the latter subclones, which is consistent with the relatively less efficient generation of the reciprocal cell types as described previously. Moreover, the clonal analysis

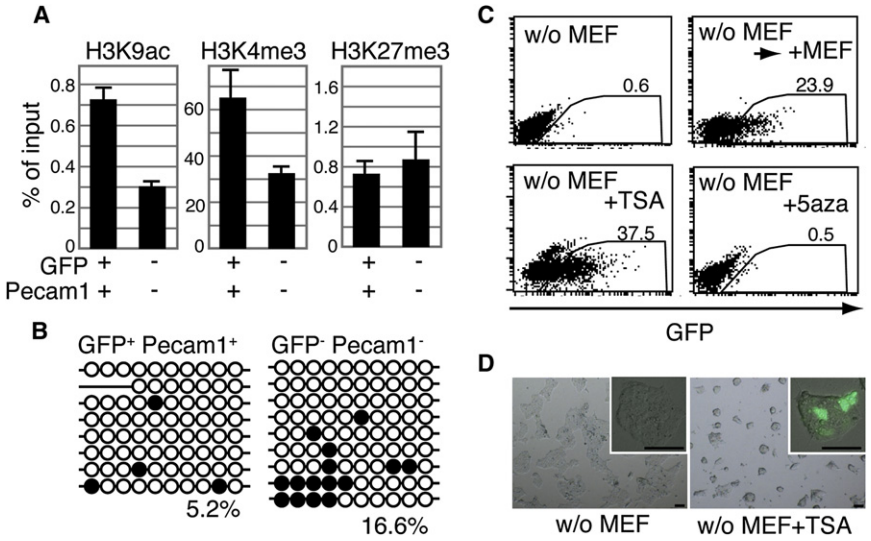

Figure 4. Epigenetic Regulaton of the *stella* Locus and Modulation of Stella-GFP-Positive Cells

(A) ChIP analysis of histone modifications in the *stella* locus. Genomic DNAs from FACS-sorted Stella-GFP-positive/Pecam1-positive or Stella-GFP-negative/Pecam1-negative cells were immunoprecipitated with the antibodies as indicated and were then subjected to Q-PCR using a primer set specific to the endogenous genomic locus encoding the start codon of Stella. Levels of histone modifications were estimated by dividing with the input value (see the Experimental Procedures).

(B) Bisulfite sequencing profiles of DNA methylation of the *stella* locus. CpG sequences are shown with filled (methylated) and open (unmethylated) circles. Gaps in the methylation profiles represent mutated or missing CpG sites. The numbers under the bisulfite sequencing profiles show the percentages of methylated CpG.

(C) FACS analysis of Stella-GFP-positive cells under various conditions. Shown are the percentages of Stella-GFP-positive cells after culturing *stella-gfp* ESCs without MEFs (upper left), followed by reculturing them on MEFs in chemically defined medium (upper right) or exposing them to TSA (lower left) or 5-aza (lower right) in the absence of MEFs.

(D) Morphology of the colonies of *stella-gfp* ESCs cultured with TSA. Images show the change in morphology of the *stella-gfp* ESC colonies cultured without MEF (left) and then following addition of TSA (right). Note the relatively more compact ESC colonies in the latter. Windows in each image represent Stella-GFP in a colony. Scale bar, 50 μm.

also showed less-efficient plating of Stella-GFP-negative/Pecam1-negative ESCs, which formed fewer colonies compared to the cells of the opposite phenotype (Figure 3D). Thus, while the overall population of Stella-positive ESCs is maintained through mutual conversion of positive and negative cells, the efficiency of the process clearly differs. We reason that the conversion of Stella-positive/Pecam1-positive cells into Stella-negative/Pecam1-negative cells follows an inherent developmental program from ICM toward epiblast, whereas the reciprocal conversion is contrary to the normal developmental program in vivo. This could account for the slower conversion rate of the latter.

Epigenetic Regulation of Metastable Stella Expression in ESCs

The intermittent expression of Stella in ESCs indicates that these pluripotent stem cells are probably in a metastable state, which should be reflected in their epigenetic states. We therefore examined histone modifications and DNA methylation in the endogenous genomic DNA sequences surrounding the start codon of Stella. We found that the Stella-GFP-positive ESCs displayed a relative enrichment of acetylated histone H3 lysine 9 (H3K9ac) and trimethylated H3K4 (H3K4me3), which are a hallmark of an active gene, compared to the levels in Stella-GFP-negative/Pecam1-negative ESCs (Figure 4A). The levels of trimethylation of H3K27 (H3K27me3), a repressive gene marker, was, however, comparable in the two populations (Figure 4A). Furthermore, the DNA sequence, which has ten CpGs, was hypomethylated in both the Stella-GFP-positive and Stella-GFP-negative/Pecam1-negative FACS-sorted cells (Figure 4B), except for a slight increase in some of the latter cells. These results indicate that the metastable expression of *stella* is regulated by chromatin-based epigenetic changes, which is independent of DNA methylation.

As the histone modifications can be relatively plastic, we next tested the responsiveness of Stella expression under a variety of conditions. First, we found that the culture of ESCs in a chemically defined medium without embryonic fibroblast feeder cells (MEFs), which are a source of signaling molecules that affect ESCs (Chambers and Smith, 2004), resulted in almost complete loss of Stella-GFP expression (Figure 4C). Notably, Stella-GFP expression was, however, restored as before in more than 20% of the ESCs when they were returned to culture with MEFs (Figure 4C). This clearly shows that the metastable state of Stella-GFP expression is influenced by environmental cues, one of which is signals from MEFs. Notably, Stella-GFP expression was also restored in response to 10 nM trichostatin A (TSA), an inhibitor of histone deacetylase, but DNA5-azacytidine, an inhibitor DNA methyltransferase, had no effect. Indeed, the proportion of Stella-GFP-positive cells increased to 37.5% in response to TSA. These ESCs also showed a striking phenotypic change as they formed compact colonies, which is characteristic of ESCs grown on MEFs (Figure 4D). These results demonstrate that histone acetylation, but not DNA methylation of Stella locus, is one of the epigenetic modifications regulating expression of Stella.

Functional Differences between the Subpopulations of ESCs

Our studies above show that the ESCs consist of subpopulations of cells that exhibit distinct gene expression profiles while being in a metastable epigenetic state. The subpopulations were in a constantly interchangeable state under conditions that maintain them in an undifferentiated state. However, we decided to investigate whether the Stella-positive/Pecam1-positive and Stella-negative/Pecam1-negative cells exhibit distinct properties if they were forced to undergo differentiation. First, we

attempted to check their differentiation potential in embryoid bodies (EBs) and found that the Stella-negative/Pecam-negative cells seldom formed EBs, whereas Stella-GFP-positive/Pecam1-positive cells could do so readily as expected and as judged by the detection of differentiation marker genes (data not shown), which suggests a difference in the properties of the two populations. Next, we cultured the two cell populations with retinoic acid (RA) that induces mainly neuronal differentiation. Q-PCR analysis showed that expression of early neuronal lineage-marker genes, *Sox1*, *Nestin*, and *Pax6*, was enhanced in Stella-GFP-negative/Pecam1-negative cells compared to the levels of expression detected in Stella-GFP-positive/Pecam1-positive cells (Figure 5A). This is not due to a difference in the basal levels of expression of these genes in each population, since *Sox1* and *Pax6* transcripts were rather lower in nonstimulated Stella-GFP-negative/Pecam1-negative cells (Figure 5A). These results demonstrate that the Stella-GFP-negative/Pecam1-negative cells were more sensitive to the signal to undergo differentiation, at least with respect to the response to RA-induced differentiation.

Next we checked their response when each population was cultured under conditions that are known to induce differentiation of trophectoderm cells (TS medium). Surprisingly, the Stella-GFP-negative/Pecam1-negative population readily exhibited remarkable upregulation of *Cdx2* gene expression, which is a marker of trophoectoerm cells in pre- and peri-implantation embryos, as well as of other markers of this lineage, such as *Hand1* and *Dlx1* (Figure 5B). Immunofluorescence analysis also showed that Cdx2 was clearly detectable in nuclei of these cells, forming dense colonies, as well as in large nuclei of presumptive trophoblast giant cells located around the periphery of differentiating colonies (Figure 5C). Recently, evidence from pluripotent stem cells derived from postimplantation epiblast cells (EpiSCs) shows that these are also more capable of differentiation into trophectoderm cells (Brons et al., 2007; Tesar et al., 2007). This is consistent with our data showing that the Stella-negative/Pecam1-negative ESCs are more like the epiblast cells. By contrast, the Stella-positive/Pecam1-positive cells failed to show this response. This is consistent with the fact that ESCs generally show a small number of differentiating trophectoderm cells when cultured under TS cell conditions. Taken together, these results demonstrate that Stella-negative cells possess functionally distinct properties, among which is a state that is permissive for differentiation into trophectoderm cells that is also observed with EpiSCs.

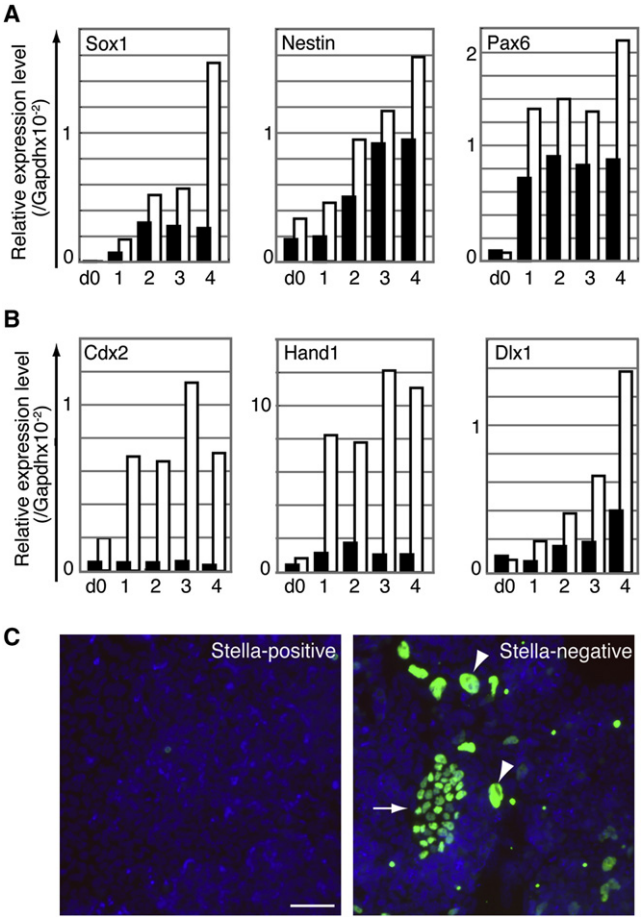

Figure 5. Differentiation Potential of Stella-Positive and Stella-Negative Populations

(A) Response to RA-induced differentiation and expression of neuronal markers. Graphs show a representative Q-PCR analysis of *Sox1*, *Nestin*, and *Pax6* expression in FACS-sorted Stella-GFP-positive/Pecam1-positive (black) and Stella-GFP-negative/Pecam1-negative (white) ESCs cultured with RA as for days (d) as indicated. Samples at d0 were prepared immediately after FACS sorting followed by RA induction.

(B) Expression of trophectoderm marker genes. Graph shows representative Q-PCR analysis of *Cdx2*, *Hand*, and *Dlx1* expression in each subpopulation, as described in (A) when cultured under TS cell conditions. Repeated Q-PCR analysis using different sets of sorted samples showed similar results as shown in both (A) and (B).

(C) Enhanced expression of Cdx2 protein. Images are immunostaining of Cdx2 (green) and DAPI (blue) in each subpopulation cultured for 3 days under TS conditions. Arrow and arrowhead indicate representative Cdx2-positive dense colony and cells having large nuclei, respectively. Scale bar, 50 μm.

Comparisons between the State of Stella in ESCs and EpiSCs

Based on our analysis, ESCs consist of a population of Stella-GFP-negative/Pecam1-negative cells that are relatively closer to the epiblast cells and share some of the differentiation potential with EpiSCs, a stem cell line from epiblast cells of postimplantation embryos. We therefore further characterized the Stella-GFP-negative/Pecam1-negative ESCs by comparing marker gene expression and epigenetic status of *stella* in EpiSCs. As expected, we detected *Fgf5* expression in EpiSCs, but the levels were significantly higher compared to those in the epiblast-like cells in ESCs (Figure 6A). By contrast, expressions of *stella*, *Pecam1*, and *Zfp42/Rex1* were negligible in EpiSCs, compared to the ESC population (Figure 6A). However, unlike a lack of *Pecam1* expression, we detected heterogeneous expression of SSEA1 in EpiSCs (Figure 6C) consistent with similar expression in the epiblast cells in vivo. Levels of *Nanog* and *Sox2* in EpiSCs are comparable to those in the epiblast-like cells in ESCs (Figure 6A). These observations suggest that the Stella-GFP-negative/Pecam1-negative population in ESCs represents an intermediate state between ICM-like cells and the EpiSCs. This was also supported by microarray analysis using single-cell gene expression profile, which revealed that ESCs with low

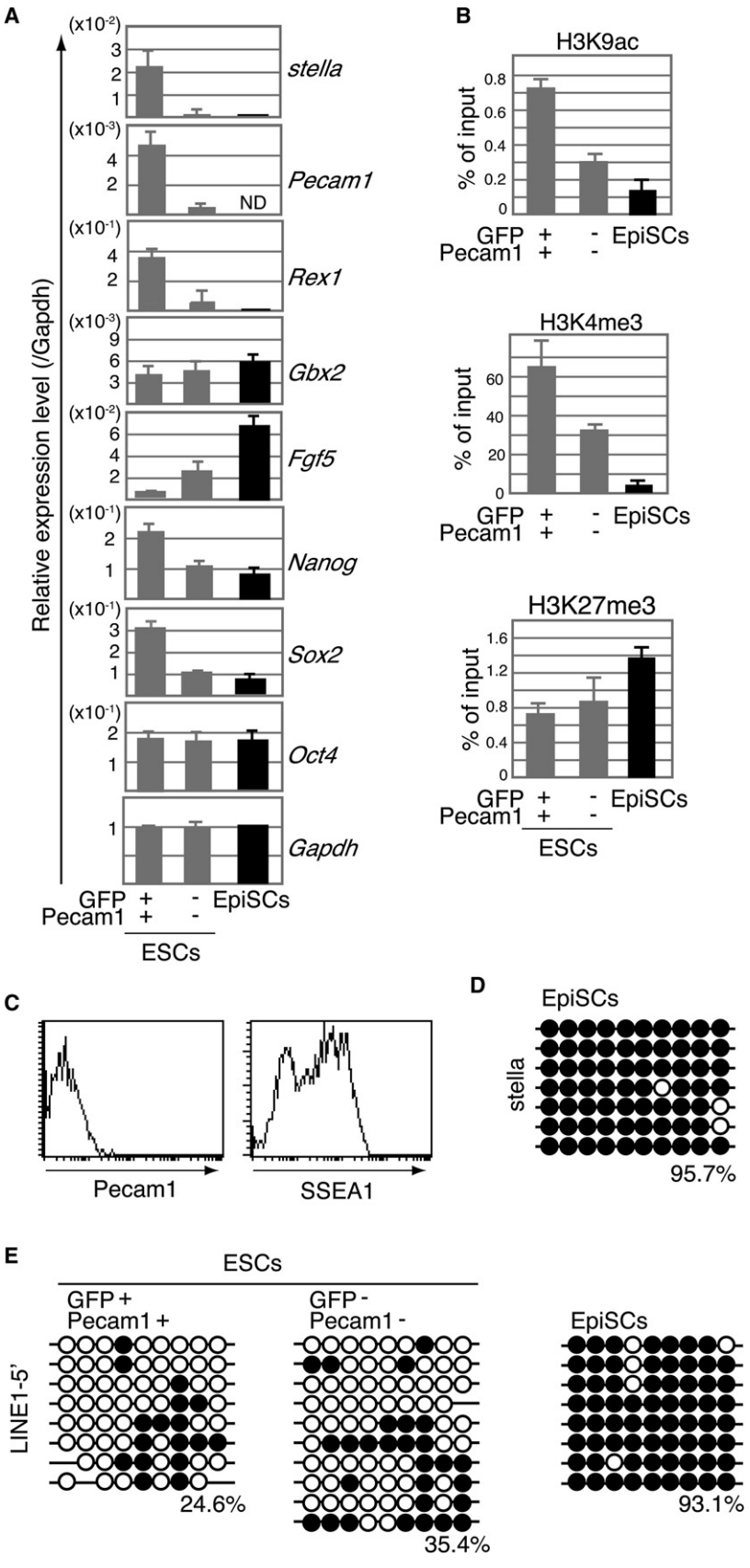

Figure 6. Distinctive Status of ESCs and EpiSCs

(A) Q-PCR analysis of gene expression in EpiSCs, FACS-sorted populations of Stella-GFP-positive and Stella-GFP-negative/Pecam1-negative ESCs. Relative levels of gene expression in EpiSCs were estimated by reference to the value of *Gapdh*.

(B) ChIP analysis of histone modifications in the *stella* locus of EpiSCs. Genomic DNAs were immunoprecipitated from FACS-sorted EpiSCs with antibodies as indicated, followed by Q-PCR analysis. Levels of histone modifications were estimated as indicated in Figure 4A.

(C) FACS analysis of Pecam1 and SSEA1 in EpiSCs. Histograms show expression of Pecam1 (left) and SSEA1 (right).

(D) Bisulfite sequencing profiles of DNA methylation in the Stella locus in EpiSCs. CpG sequences are shown with filled (methylated) and open (unmethylated) circles.

(E) Bisulfite sequencing profiles of LINE-1. Sequences are shown with filled (methylated) and open (unmethylated) circles. The numbers under the bisulfite sequencing profiles show the percentages of methylated CpG. Gaps in the methylation profiles represent mutated or missing CpG sites. The numbers under the bisulfite sequencing profiles show the percentages of methylated CpG.

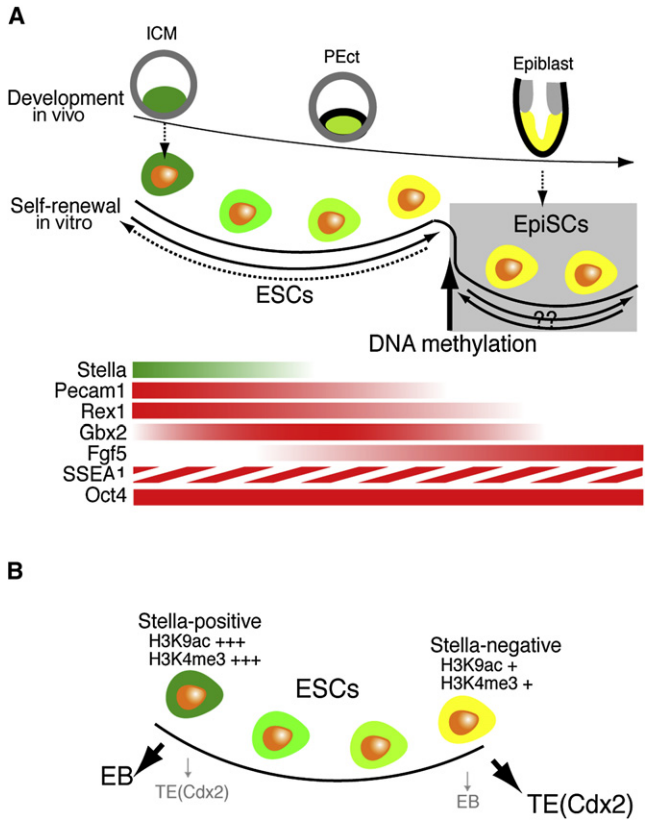

Figure 7. Proposed Model for the Maintenance in ESCs Composed of Distinct Cell Types in a Dynamic Equilibrium

(A) ESCs are represented as consisting of distinct subpopulations of cells, each of which has a different combination of developmentally regulated genes spanning between the ICM and epiblast-like phenotype. The mechanism that drives ESCs from ICM to epiblast-like cells may be similar to that which regulates the inherent developmental program from ICM of blastocysts to epiblast of postimplantation embryos in vivo, but the mechanism involved in the reverse process of epiblast-like cells back to ICM-like cells suggests a dedifferentiation step (broken line); the mechanism regulating the latter is unknown. The region representing self-renewal of ESCs is distinct from that which governs self-renewal of EpiSCs. Notably, DNA methylation of the *stella* locus is one criteria that distinguishes ESCs from EpiSCs (see text for details).

(B) Distinct functional and epigenetic states of the two major subpopulations detected in ESCs. Expression of *stella* in ESCs is regulated by distinct histone-based epigenetic modifications. Stella-positive and Stella-negative subpopulations also exhibit characteristic functional differences; the latter possess the potential for differentiation into trophectoderm cells (TE) but show poor ability to form embryoid bodies (EB) from single cells as seen with EpiSCs. By contrast, Stella-positive cells can readily form EBs from single cells but show little if any tendency to differentiate into TE. (See text for details.)

expression of *stella* had an intermediate gene expression profile when compared with ESCs with high expression of *stella* and EpiSCs (Figure S2). In other words, cells with low expression of *stella* were closer to the EpiSCs compared to the cells with high expression of *stella*.

Next we compared the epigenetic status of *stella* locus in EpiSCs with the situation in ESCs. Compared to epiblast-like cells in ESCs, the levels of H3K9ac and H3K4me3 in EpiSCs were considerably diminished (Figure 6B), whereas that of H3K27me3 showed an increase. Most strikingly, the *stella* locus showed extensive DNA methylation in EpiSCs (Figure 6D). These results demonstrate that the epigenetic status and regulation of *stella* in the epiblast-like ESC subpopulations and EpiSCs differ significantly. Apart from the *stella* locus, LINE1 sequences, a retrotransposable element that is widely distributed in the genomic DNA, were also hypermethylated in EpiSCs, whereas they were hypomethylated in both populations from ESCs (Figure 6E), which demonstrates that DNA methylation takes place not only in the *stella* locus but also in genome-wide regions. These observations are consistent with the fact that de novo DNA methylation takes place in the pluripotent cell population in vivo during peri-implantation development (Kafri et al., 1992; Monk et al., 1987), which is essential for further development (Li et al., 1992; Okano et al., 1999). DNA methylation at this stage is linked to the incipient differentiation of pluripotent cells involving developmentally regulated genes, one of which is *stella*.

DISCUSSION

Single-cell analysis demonstrates that ESCs exhibit heterogeneity that spans across ICM to epiblast-like phenotypes. Whereas expression of *stella* in ESCs represents one extreme of ICM-like cells, the mutually exclusive expression of *Fgf5* among Stella-GFP-negative/*Pecam1*-negative cells represents the most epiblast-like cells. Thus, ESCs are not a homogeneous group of self-renewing cells as they constantly fluctuate between ICM and epiblast-like states with an apparent adherence to an inherent program. Since the number of cells with *stella* transcripts exceeds those that exhibit endogenous Stella and Stella-GFP, it is possible that translational regulation mechanisms may be important during self-renewal and pluripotency. The expression of *stella* in ESCs is regulated by histone-based modifications, which is responsive to environmental and epigenetic factors. By contrast, *stella* in EpiSCs derived from the postimplantation epiblast cells is repressed robustly by DNA methylation, which denotes a barrier between the two types of pluripotent stem cells (Figure 7A).

It was striking that the proportion of Stella-GFP-positive cells in ESCs remained relatively constant, even after the culture of Stella-GFP-positive/Pecam1-positive and Stella-GFP-negative/Pecam1-negative cells separately, as they regenerated the appropriate number of reciprocal cell types. However, the latter were slower than the former in converting into the reciprocal cell types. This is presumably because in the first case, the cells are progressing along an inherent developmental program from ICM- toward epiblast-like cells, while the converse represents a "dedifferentiation" step that is contrary to the normal developmental program. Our single-cell analysis also shows that cells lacking in *stella* transcripts had exceedingly low levels of *Pecam1* expression as well as lower levels of *nanog* expression. These observations are broadly in agreement with the differential expression of Pecam1 in ESCs, where the Pecam1-negative cells are predominantly epiblast-like cells (Furusawa et al., 2006; Kemp et al., 2005). Furthermore, Pecam1-positive or Nanog-positive cells constitute a relatively stable population of ESCs (Chambers et al., 2007; Furusawa et al., 2006; Furusawa et al., 2004), while the Pecam1-negative and Nanog-negative cells are harder to convert back into their reciprocal counterparts.

Consistent with the interchangeability of ESCs, we found that the proportion of Stella-GFP-positive cells was reversibly responsive to MEFs, which are a source of signaling molecules that may in turn influence the intrinsic epigenetic state of responding cells (Ansel et al., 2003; Kang et al., 2005; van Grunsven et al., 2005). Multiple signaling molecules, together with the transcription and epigenetic factors, play an essential role in maintaining pluripotency in ESCs (Chambers and Smith, 2004; Surani et al., 2007). We stress that the proportion of Stella-GFP-positive cells could significantly exceed those we report here, provided appropriate conditions exist that promote the ICM-like phenotype. Indeed, ESCs cultured without MEFs that were almost completely in an epiblast-like state showed a very significant increase in Stella-GFP-positive cells in response to TSA. Thus, TSA-induced reprogramming of ESCs caused a significant shift toward an ICM-like state from a virtual epiblast-like state prior to the treatment. Notably, the effect of TSA was striking because it also induced a marked phenotypic change in the ESCs colonies, which acquired an appearance that is reminiscent of the colonies grown on MEFs. Consistently, it was reported that the same concentration (10 nM) of TSA inhibited differentiation of ESCs when cultured without LIF (Lee et al., 2004), although a significantly higher dosage of TSA induced ESC differentiation (McCool et al., 2007). Thus, the balance between histone acetylation and deacetylation may be at least one factor that may determine whether ESCs are in an ICM-like or epiblast-like state.

The gene expression profile indicated that the *stella*-negative ESCs are situated between ICM and fully developed epiblasts. Under the culture conditions that maintain ESCs, the *stella*-negative cells might not be able to progress to the EpiSCs owing to the extrinsic signals that force them back to the ICM-like state. However, when Stella-GFP-negative/Pecam1-negative ESCs were cultured under EpiSC condition, *Fgf5* expression showed a further increase (data not shown). More importantly, we demonstrate that the Stella-positive and Stella-negative cells show clear differences with respect to their potential for differentiation (Figure 7B). Notably, the Stella-negative cells can differentiate into trophectoderm cells, a property they share with EpiSCs. Analysis of epigenetic status, however, clearly showed that DNA methylation of the *stella* locus represents a boundary between ESCs and EpiSCs. EpiSCs, despite showing expression of pluripotent marker genes including *Oct4*, *Sox2*, and *Nanog*, are epigenetically quite distinct from ESCs, as they rarely contribute to chimeras, and unlike ESCs, they exhibit an inactive X chromosome (Tesar et al., 2007). Notably, the EpiSCs do not exhibit an ICM-like state unlike ESCs, which can fluctuate freely within the ''self-renewal parameters'' encompassed by the ICM and epiblast-like states and where *stella* locus is hypomethylated and its expression is regulated by chromatin-based modifications (Figure 7A). Furthermore, this is consistent with the evidence that de novo DNA methylation is not essential for self-renewal of ESCs but is essential for their differentiation (Chen et al., 2003; Lei et al., 1996).

Our preliminary evidence shows that the *stella* locus in EpiSCs is subject to DNA demethylation only in the cells that undergo specification into PGCs (K.H. and M.A.S., unpublished data), consistent with the fact that Stella is only expressed in the germ cell lineage after implantation (Saitou et al., 2002; Sato et al., 2002). This epigenetic change in the *stella* locus exclusively in PGCs is probably an important hallmark of other significant epigenetic reprogramming events in PGCs. Strikingly, these epigenetic changes in PGCs confer the ability on early germ cells to undergo dedifferentiation into pluripotent embryonic germ cells, which resemble ESCs. EpiSCs themselves may lack the ability to convert directly into ESCs with a population of ICM-like cells.

In view of our findings, it is striking to note a virtual loss of *stella* expression in ESCs with a null mutation in the gene encoding methyl-CpG-binding domain protein 3 (Mbd3), which is a member of the NuRD complex (Kaji et al., 2006). Reciprocally, the *Mbd3* null ESCs show high levels of *Fgf5* expression, possibly as they acquire a more epiblast-like character and grow independently of LIF, although they are unable to differentiate. Mbd3 is also essential for peri-implantaton development in vivo. Similarly, *Dicer* null ESCs can be maintained without LIF, but they are impaired in their ability to undergo differentiation (Kanellopoulou et al., 2005; Murchison et al., 2005). We predict that these mutant cells may be more epiblast-like and devoid of Stella expression, and their differentiation is impaired because of attenuated DNA methylation due to misexpression of de novo DNA methyltransferases (Sinkkonen et al., 2008). Thus, the exit from ESCs and loss of ICM-like *stella*-positive phenotype is coupled with DNA methylation as represented by methylation of the *stella* locus.

In conclusion, our study shows that ESCs are not a group of uniform self-renewing cells, since they appear to be in a metastable state and shift between ICM- and epiblast-like states while retaining pluripotency. This equilibrium can shift in either direction in response to a variety of factors, including epigenetic regulators. Analysis of Stella expression may be used to determine the precise phenotypic state of different ESC lines and of the factors, including epigenetic regulators, that affect its expression. The proportion of Stella-GFP-positive, and therefore ICM-like, cells in ESC cultures is a sensitive indicator of optimal environmental or epigenetic modulators that promote this phenotypic state. Further studies may also reveal the precise role of Stella in the derivation and maintenance of ESCs.

EXPERIMENTAL PROCEDURES

Cell Culture

ESCs were grown in ESC medium (DMEM/F12, Invitrogen; supplemeted with 15% fetal calf serum, 1 mM glutamine, 100 u/ml penicillin/streptomycin, 0.1 mM β-mercaptoethanol, and 1000 u/ml LIF) on mitomycin C-treated MEFs, unless specifically mentioned. For clonal culture analysis, 500 FACS-sorted single ESCs were spread on MEFs seeded on 6 cm tissue culture dish. After 5 days of culture, the number of colonies on the dish was counted, and then the colonies were picked up, trypsinised, and transferred into 24-well dishes. At 4 days after picking the colonies up, Stella-GFP-positive cells were analyzed by FACS. To establish MEF-independent *stella-gfp* ESCs, the ESC line was cultured in Clonal Grade Medium (Chemicon) for 10–14 days and then maintained in knockout DMEM (Invitrigen) containing 20% of knockout serum replacement, 1 mM glutamine, 100 u/ml penicillin/streptomycin, 0.1 mM β-mercaptoethanol, and 1000 u/ml LIF. The KSR-containing medium was used as the chemically defined medium. For differentiation analysis, FACS-sorted cells (1×10^5cells/ml) were cultured in the chemically defined medium with RA (1 μM) or in TS medium with supernatant from medium cultured with MEFs (Tanaka et al., 1998). For EB formation, cells were seeded into Petri dish in medium without LIF. EpiSCs were cultured in N2B27 supplemented

with 20% KSR, 2 ng/ml of recombinant human Activin A (Peprotech), and 12 ng/ml of bFGF (Invitrogen). Both ESCs and EpiSCs were cultured in 5% CO_2/95% air at 37°C.

FACS and Immunofluorescence Analysis

For FACS analysis, single-cell suspension was stained with R-Phycoerythrin-conjugated rat anti-Pecam1 (BD Pharmingen) and anti-SSEA1 antibody (TG1). The stained cells were analyzed and sorted by FACSort with CELLQUEST software (BD Biosciences) and FACSAria (BD Biosciences), respectively. Immunofluorescence analysis of cells was performed essentially as described (de Sousa Lopes et al., 2004; Ohinata et al., 2005). The antibodies used were rabbit anti-PGC7/Stella, mouse anti-CDX2 (Cdx2-88, BioGenex), and rat anti-GFP (Nacalai tesque). All secondary antibodies used were Alexa Fluor highly crossed adsorbed (Molecular Probes). Samples were mounted in Vectashield with DAPI (Vector). Immunofluorescence signals were detected by an Olympus IX71 inverted microscope or by a Bio-Rad (Hercules, CA) Radiance 2000 confocal microscope.

RT-PCR Analysis

For Q-PCR analysis using fractionated cells, total RNA was extracted from sorted ESCs and EpiSCs by using Trizol (Sigma). cDNA was synthesized using Superscript II and oligo d(T) primer (Invitrogen) followed by Q-PCR reaction using SYBR Green master mix (QIAGEN) and specific primers. For Q-PCR using single cells, single-cell cDNA preparation was performed as described in detail previously (Kurimoto et al., 2007). The putative number of transcripts was estimated by referring in vitro-transcribed control transcripts (Kurimoto et al., 2007). cDNAs was used for each 20 μl Q-PCR reaction with SYBR Green Master Mix (QIAGEN) and 1 μM of each primer and was amplified under the following conditions: 95°C for 10 min and then 40 cycles of 95°C for 15 s and 60°C for 1 min. Primer sequences used in this study are available on request.

CHIP Analysis

FACS-sorted 10^6 ESCs or EpiSCs and 3×10^7 3T3 cells, as carrier cells, were fixed with 1% formaldehyde, lysed, and sonicated to obtain 200–500 bp DNA fragments conjugated with nucleosomes. The sonicated lysates were immunoprecipitated with rabbit polyclonal anti-acetyl H3K9 (Abcam), mouse monoclonal anti-trimethyl H3K4 (Abcam), or rabbit polyclonal anti-tri-methyl H3K27 (Abcam) antibodies that were in advance reacted with secondary antibodies conjugated with magnetic beads (Dynal). After incubation with each antibody for 1 day, immunoprecipitants were recovered and washed by using magnetic stand (Dynal). Then DNA fragments contained in the immunoprecipitants were purified by incubation with Proteinase K. The DNA fragments were subjected to Q-PCR. Whole-cell lysates before incubation with antibodies were used as input. DNA fragments from whole lysates and immunoprecipitants were subject to pre-PCR at 15 and 20 cycles, respectively. After purifying the pre-PCR products by PCR purification kit, 1 μl of the product was used for Q-PCR reaction 1 μM of nested primers. Negative control samples using only secondary antibodies conjugated with magnetic beads showed similar levels of very low background or no detectable background. Primer sequences used in this study are available on request.

Bisulfite Sequence Analysis

Bisulphite sequence analysis of the genomic DNA isolated from FACS-sorted ESCs was carried out by EpiTect Bisulfite Kit (QIAGEN). The primer sequences and PCR conditions for amplification of LINE1 and IAP sequences are previously described (Lane et al., 2003). The PCR products were cloned using pGEM-T Easy Vector System I (Promega) and were sequenced by Cogenics.

SUPPLEMENTAL DATA

The Supplemental Data include two figures, Supplemental Experimental Procedures, and Supplemental References and can be found with this article online at http://www.cellstemcell.com/cgi/content/full/3/4/391/DC1/.

ACKNOWLEDGMENTS

We are grateful to T. Nakano for anti-PGC7 and P. Beverly for mouse anti-SSEA1. We thank C. Lee for technical support; C. Mummery for continuing support; and A. McLaren, B. Payer, P. Hajkova, and S. Jeffries for useful comments on the manuscript. This work was supported by the Netherlands Organization for Scientific Research (NWO, TALENT 809.67.024) to S.M.C.S.L.; the Japan Society for Promotion of Science to K.H.; and The Technology Programme (DTI Project Number TP/4/BIO/6/I/22020) of CellCentric Ltd and The Technology Strategy Board sponsored by the Department for Innovation, Universities, and Skills (DIUS); and the Wellcome Trust (062801).

Received: May 8, 2007
Revised: April 28, 2008
Accepted: July 29, 2008
Published: October 8, 2008

REFERENCES

Ansel, K.M., Lee, D.U., and Rao, A. (2003). An epigenetic view of helper T cell differentiation. Nat. Immunol. *4*, 616–623.

Avilion, A.A., Nicolis, S.K., Pevny, L.H., Perez, L., Vivian, N., and Lovell-Badge, R. (2003). Multipotent cell lineages in early mouse development depend on SOX2 function. Genes Dev. *17*, 126–140.

Brons, I.G., Smithers, L.E., Trotter, M.W., Rugg-Gunn, P., Sun, B., Chuva de Sousa Lopes, S.M., Howlett, S.K., Clarkson, A., Ahrlund-Richter, L., Pedersen, R.A., and Vallier, L. (2007). Derivation of pluripotent epiblast stem cells from mammalian embryos. Nature *448*, 191–195.

Chambers, I., and Smith, A. (2004). Self-renewal of teratocarcinoma and embryonic stem cells. Oncogene *23*, 7150–7160.

Chambers, I., Colby, D., Robertson, M., Nichols, J., Lee, S., Tweedie, S., and Smith, A. (2003). Functional expression cloning of Nanog, a pluripotency sustaining factor in embryonic stem cells. Cell *113*, 643–655.

Chambers, I., Silva, J., Colby, D., Nichols, J., Nijmeijer, B., Robertson, M., Vrana, J., Jones, K., Grotewold, L., and Smith, A. (2007). Nanog safeguards pluripotency and mediates germline development. Nature *450*, 1230–1234.

Chapman, G., Remiszewski, J.L., Webb, G.C., Schulz, T.C., Bottema, C.D., and Rathjen, P.D. (1997). The mouse homeobox gene, Gbx2: genomic organization and expression in pluripotent cells in vitro and in vivo. Genomics *46*, 223–233.

Chen, T., Ueda, Y., Dodge, J.E., Wang, Z., and Li, E. (2003). Establishment and maintenance of genomic methylation patterns in mouse embryonic stem cells by Dnmt3a and Dnmt3b. Mol. Cell. Biol. *23*, 5594–5605.

Clark, A.T., Rodriguez, R.T., Bodnar, M.S., Abeyta, M.J., Cedars, M.I., Turek, P.J., Firpo, M.T., and Reijo Pera, R.A. (2004). Human STELLAR, NANOG, and GDF3 genes are expressed in pluripotent cells and map to chromosome 12p13, a hotspot for teratocarcinoma. Stem Cells *22*, 169–179.

Cui, L., Johkura, K., Yue, F., Ogiwara, N., Okouchi, Y., Asanuma, K., and Sasaki, K. (2004). Spatial distribution and initial changes of SSEA-1 and other cell adhesion-related molecules on mouse embryonic stem cells before and during differentiation. J. Histochem. Cytochem. *52*, 1447–1457.

de Sousa Lopes, S.M., Roelen, B.A., Monteiro, R.M., Emmens, R., Lin, H.Y., Li, E., Lawson, K.A., and Mummery, C.L. (2004). BMP signaling mediated by ALK2 in the visceral endoderm is necessary for the generation of primordial germ cells in the mouse embryo. Genes Dev. *18*, 1838–1849.

Furusawa, T., Ohkoshi, K., Honda, C., Takahashi, S., and Tokunaga, T. (2004). Embryonic stem cells expressing both platelet endothelial cell adhesion molecule-1 and stage-specific embryonic antigen-1 differentiate predominantly into epiblast cells in a chimeric embryo. Biol. Reprod. *70*, 1452–1457.

Furusawa, T., Ikeda, M., Inoue, F., Ohkoshi, K., Hamano, T., and Tokunaga, T. (2006). Gene expression profiling of mouse embryonic stem cell subpopulations. Biol. Reprod. *75*, 555–561.

Kafri, T., Ariel, M., Brandeis, M., Shemer, R., Urven, L., McCarrey, J., Cedar, H., and Razin, A. (1992). Developmental pattern of gene-specific DNA methylation in the mouse embryo and germ line. Genes Dev. *6*, 705–714.

Kaji, K., Caballero, I.M., MacLeod, R., Nichols, J., Wilson, V.A., and Hendrich, B. (2006). The NuRD component Mbd3 is required for pluripotency of embryonic stem cells. Nat. Cell Biol. *8*, 285–292.

Kanellopoulou, C., Muljo, S.A., Kung, A.L., Ganesan, S., Drapkin, R., Jenuwein, T., Livingston, D.M., and Rajewsky, K. (2005). Dicer-deficient mouse embryonic stem cells are defective in differentiation and centromeric silencing. Genes Dev. *19*, 489–501.

Kang, J., Shi, Y., Xiang, B., Qu, B., Su, W., Zhu, M., Zhang, M., Bao, G., Wang, F., Zhang, X., et al. (2005). A nuclear function of beta-arrestin1 in GPCR signaling: regulation of histone acetylation and gene transcription. Cell *123*, 833–847.

Kemp, C., Willems, E., Abdo, S., Lambiv, L., and Leyns, L. (2005). Expression of all Wnt genes and their secreted antagonists during mouse blastocyst and postimplantation development. Dev. Dyn. *233*, 1064–1075.

Kurimoto, K., Yabuta, Y., Ohinata, Y., Ono, Y., Uno, K.D., Yamada, R.G., Ueda, H.R., and Saitou, M. (2006). An improved single-cell cDNA amplification method for efficient high-density oligonucleotide microarray analysis. Nucleic Acids Res. *34*, e42. Published online March 17, 2006. 10.1093/nar/gkl050.

Kurimoto, K., Yabuta, Y., Ohinata, Y., and Saitou, M. (2007). Global single-cell cDNA amplification to provide a template for representative high-density oligonucleotide microarray analysis. Nat. Protocols *2*, 739–752.

Lane, N., Dean, W., Erhardt, S., Hajkova, P., Surani, A., Walter, J., and Reik, W. (2003). Resistance of IAPs to methylation reprogramming may provide a mechanism for epigenetic inheritance in the mouse. Genesis *35*, 88–93.

Lee, J.H., Hart, S.R., and Skalnik, D.G. (2004). Histone deacetylase activity is required for embryonic stem cell differentiation. Genesis *38*, 32–38.

Lei, H., Oh, S.P., Okano, M., Juttermann, R., Goss, K.A., Jaenisch, R., and Li, E. (1996). De novo DNA cytosine methyltransferase activities in mouse embryonic stem cells. Development *122*, 3195–3205.

Li, E., Bestor, T.H., and Jaenisch, R. (1992). Targeted mutation of the DNA methyltransferase gene results in embryonic lethality. Cell *69*, 915–926.

McCool, K.W., Xu, X., Singer, D.B., Murdoch, F.E., and Fritsch, M.K. (2007). The role of histone acetylation in regulating early gene expression patterns during early embryonic stem cell differentiation. J. Biol. Chem. *282*, 6696–6706.

Monk, M., Boubelik, M., and Lehnert, S. (1987). Temporal and regional changes in DNA methylation in the embryonic, extraembryonic and germ cell lineages during mouse embryo development. Development *99*, 371–382.

Murchison, E.P., Partridge, J.F., Tam, O.H., Cheloufi, S., and Hannon, G.J. (2005). Characterization of Dicer-deficient murine embryonic stem cells. Proc. Natl. Acad. Sci. USA *102*, 12135–12140.

Ohinata, Y., Payer, B., O'Carroll, D., Ancelin, K., Ono, Y., Sano, M., Barton, S.C., Obukhanych, T., Nussenzweig, M., Tarakhovsky, A., et al. (2005). Blimp1 is a critical determinant of the germ cell lineage in mice. Nature *436*, 207–213.

Okano, M., Bell, D.W., Haber, D.A., and Li, E. (1999). DNA methyltransferases Dnmt3a and Dnmt3b are essential for de novo methylation and mammalian development. Cell *99*, 247–257.

Payer, B., Chuva de Sousa Lopes, S.M., Barton, S.C., Lee, C., Saitou, M., and Surani, M.A. (2006). Generation of stella-GFP transgenic mice: a novel tool to study germ cell development. Genesis *44*, 75–83.

Pelton, T.A., Sharma, S., Schulz, T.C., Rathjen, J., and Rathjen, P.D. (2002). Transient pluripotent cell populations during primitive ectoderm formation: correlation of in vivo and in vitro pluripotent cell development. J. Cell Sci. *115*, 329–339.

Pesce, M., Gross, M.K., and Scholer, H.R. (1998). In line with our ancestors: Oct-4 and the mammalian germ. Bioessays *20*, 722–732.

Rathjen, J., Lake, J.A., Bettess, M.D., Washington, J.M., Chapman, G., and Rathjen, P.D. (1999). Formation of a primitive ectoderm like cell population, EPL cells, from ES cells in response to biologically derived factors. J. Cell Sci. *112*, 601–612.

Robson, P., Stein, P., Zhou, B., Schultz, R.M., and Baldwin, H.S. (2001). Inner cell mass-specific expression of a cell adhesion molecule (PECAM-1/CD31) in the mouse blastocyst. Dev. Biol. *234*, 317–329.

Saitou, M., Barton, S.C., and Surani, M.A. (2002). A molecular programme for the specification of germ cell fate in mice. Nature *418*, 293–300.

Sato, M., Kimura, T., Kurokawa, K., Fujita, Y., Abe, K., Masuhara, M., Yasunaga, T., Ryo, A., Yamamoto, M., and Nakano, T. (2002). Identification of PGC7, a new gene expressed specifically in preimplantation embryos and germ cells. Mech. Dev. *113*, 91–94.

Sinkkonen, L., Hugenschmidt, T., Berninger, P., Gaidatzis, D., Mohn, F., Artus-Revel, C.G., Zavolan, M., Svoboda, P., and Filipowicz, W. (2008). MicroRNAs control de novo DNA methylation through regulation of transcriptional repressors in mouse embryonic stem cells. Nat. Struct. Mol. Biol. *15*, 259–267.

Surani, M.A., Hayashi, K., and Hajkova, P. (2007). Genetic and epigenetic regulators of pluripotency. Cell *128*, 747–762.

Tanaka, S., Kunath, T., Hadjantonakis, A.K., Nagy, A., and Rossant, J. (1998). Promotion of trophoblast stem cell proliferation by FGF4. Science *282*, 2072–2075.

Tesar, P.J., Chenoweth, J.G., Brook, F.A., Davies, T.J., Evans, E.P., Mack, D.L., Gardner, R.L., and McKay, R.D. (2007). New cell lines from mouse epiblast share defining features with human embryonic stem cells. Nature *448*, 196–199.

Toyooka, Y., Shimosato, D., Murakami, K., Takahashi, K., and Niwa, H. (2008). Identification and characterization of subpopulations in undifferentiated ES cell culture. Development *135*, 909–918.

van Grunsven, L.A., Verstappen, G., Huylebroeck, D., and Verschueren, K. (2005). Smads and chromatin modulation. Cytokine Growth Factor Rev. *16*, 495–512.

Ying, Q.L., Nichols, J., Chambers, I., and Smith, A. (2003). BMP induction of Id proteins suppresses differentiation and sustains embryonic stem cell self-renewal in collaboration with STAT3. Cell *115*, 281–292.

Zwaka, T.P., and Thomson, J.A. (2005). A germ cell origin of embryonic stem cells? Development *132*, 227–233.